SPARK COUNTER WITH A LOCALIZED DISCHARGE

G.V.Fedotovich, Yu.N.Pestov and
K.N.Putilin

Institute of Nuclear Physics,
630090, Novosibirsk 90, USSR

Summary

The principle of operation of spark counter with a localized discharge are described from the view point of the improvement of its time characteristics. The application results of these counters in the experiment at the colliding beam facility VEPP-2M and status of the spark counter program in Novosibirsk are discussed.

Introduction

We see two main application of spark counters with a localized discharge [1] in detectors for experiments at colliding beam facilities: 1) precise time measurements for the particle identification by TOF and 2) an application in the electromagnetic shower and hadron calorimeters for the energy, coordinate and time measurements. The advantages of these spark counters compared to others gaseous detectors and scintillation counters are the high time resolution (~ 10 times better than that for scintillation counters) and the same accuracy in position measurements as that in the case of drift chambers. The pulse amplitudes of few volts and a rise time ~ 0.1 ns simplifies the electronics.

The operation principle of these counters will be described from the view point of improvement of its time characteristics. The results of the application of the counters in the colliding beam experiments at the VEPP-2M facility and the spark counter program status in Novosibirsk are discussed.

1. Spark Counter with a Localized Discharge

The spark counter with a localized discharge consists of two plane - parallel electrodes separated from each other by a gas gap. These electrodes are supplied with a constant voltage above the threshold value at which the particles begin to induce discharges between the electrodes. The sparks discharge a limited area of electrodes. The radius of this region is of the order of the spark gap size. Under these conditions the sensitivity to the particles situated on the remaining counter area is preserved. Discharge location is achieved by using semiconductive glass with high resistivity (10^9 + + $10^{10}\,\Omega$.cm) for one of the counter electrodes and choosing a special gas mixture which absorbs photons prior to their travelling to the regions of the high electric field [2].

A principal lay-out of the counter is shown in Fig. 1. The anode is made of the semiconductive glass and the cathode is an ordinary glass onto which a layer of copper is vacuum-deposited. A typical gas mixture consists of a noble gas with an addition of

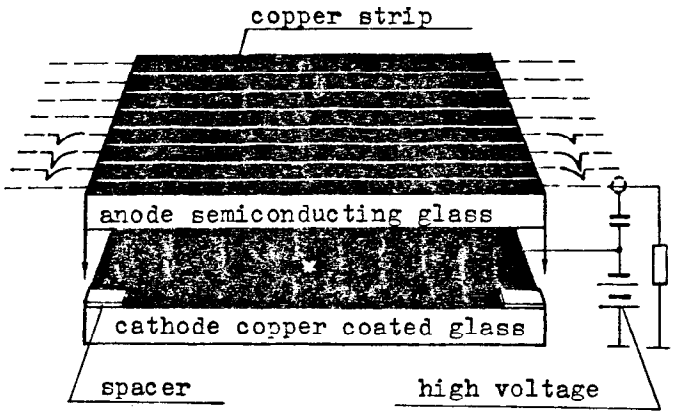

Fig. 1 The principal lay-out of the localized discharge spark counter.

organic gases whose total absorption spectra cover a wide range of photon wavelengths below 225 nm: 2.5% 1.3 butadiene; 1.9% ethylene; 10% isobutane; and 85.6% argon under a total pressure of 12 atmospheres (Fig. 2).

The signals propagate in both directions of the counter along the strip transmission lines formed by the cathode and conductive strips 10 mm wide. These copper strips are deposited onto the high-resistivity electrode's surface opposite to the spark gap (Fig.1). The pulse amplitude is several volts at a load of 50 Ω. The arrival times of the signals from the opposite ends of the counter τ_1 and τ_2 provide information on the time of particle passage $((\tau_1+\tau_2)/2)$ and

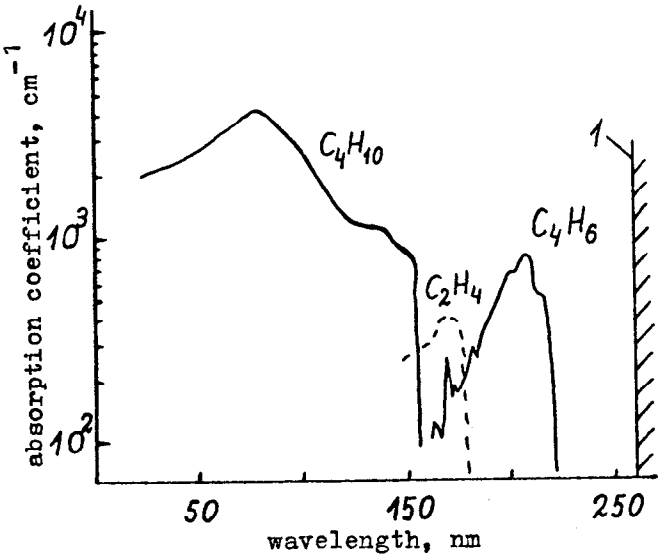

Fig. 2 Photon absorption coefficient for gas mixture used in spark counter: 1 - red boundary of the photoeffect for copper.

the coordinate along the strip lines $((\tau_1 - \tau_2)/2)$. The transverse coordinate may be determined by using the standard procedures for finding the centre of gravity of the signals induced on strips.

Counters have been constructed with areas up to 30 cm x 30 cm and with the 1.0,0.2 was achieved at a gap of 0.1 mm and was σ_τ = 24 ps. The accuracy of the coordinate along the counter's strips is measured to be equal to $\simeq$ 0.2 mm.

2. Some possible ways of improvement of the counter time characteristics

According to streamer's theory, electron in the strong electric field quicly avalanches, and this process can be described by

$$N = e^{\alpha X} \qquad (1)$$

where X is the distance from the start point of an avalanche, and α - the first Townsend coefficient [3]

$$\alpha = Ap \cdot EXP(-BP/E) \qquad (2)$$

where A and B are the constants dependig on gas mixture; P,E are the applied gas pressure and electric field.

When the number of electrons $N_{cr} \sim 10^8$ ($\alpha X \sim 20$), an avalanche turns into streamer, which quickly bridges the counter gap [3]. Hense the time delay from single electron is defined by formula

$$t_D^{(1)} = \frac{20}{\alpha v} \qquad (3)$$

where v is the electron drift velocity.

The delay time fluctuation is defined by the fluctuations both of gaseous amplification and transition moment from avalanche to streamer. Both of them are proportional to the delay time and therefore, the total time resolution is equal to

$$\sigma_\tau^{(1)} = a \cdot t_D = a \cdot \frac{20}{\alpha v} = \frac{b}{\alpha v} \qquad (4)$$

where a and b are proportional coefficients.

In the gas of counter relativistic particle creates on average, N_0 (1/cm) of primary electrons. If the average distance between them is more than the characteristic length $1/\alpha$ where the avalanche growth by "e", then it is possible to consider the development of avalanches independetly.

The situation in the counters is close to this case as

$$1/N_0 \sim 25\,\mu m \gg 1/\alpha \sim 2 \div 4\,\mu m.$$

The delay time fluctuations are determined by the transition moment from the first (in time) avalanche to the streamer. In this case, the distribution of discharge delay time can be written by the formula

$$F(t) = \sum_{N=1}^{\infty} \frac{\bar{N}^N e^{-\bar{N}} N}{N!(1-e^{-\bar{N}})} \phi(t) \left[\int_t^\infty \phi(t')dt'\right]^{N-1} =$$

$$= \frac{\bar{N}}{(e^{\bar{N}}-1)} \phi(t) \cdot EXP\left[\bar{N} \cdot \int_t^\infty \phi(t')dt'\right] \qquad (5)$$

where $\phi(t)$ is the delay time distribution for a single electron; N - the number of electrons, with the average number of primary electrons $\bar{N}$, which may cause the discharge in the gap. The calculations performed for the distribution (5) with the normal curve [4] for $\phi(t)$ and the same with

$$\phi(t) = \frac{1}{2} EXP(-|t|) \qquad (6)$$

vary slower compared with $\sqrt{\bar{N}}$ dependence of the delay time fluctuation on $\bar{N}$ (Fig. 3).

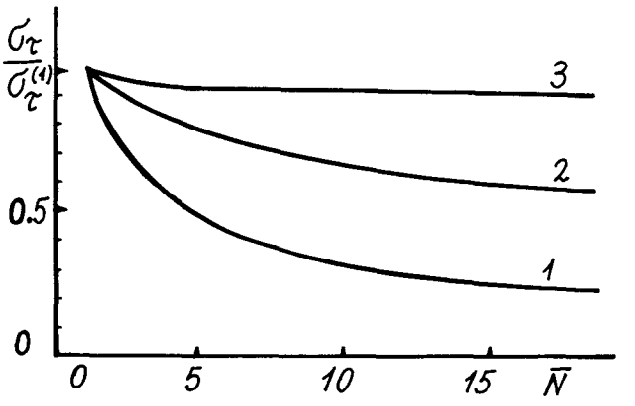

Fig. 3 The time resolution dependence on the number of primary ion pairs: (1) $\sigma_\tau/\sigma_\tau^1 = 1/\sqrt{\bar{N}}$; (2) the calculation of Eq. (5) with $f(t) = \exp(-t^2/2)/\sqrt{2\pi}$; and (3) the same with $f(t) = \exp(-|t|)^2/2$.

The comparison of time resolution for various number of initial ion pairs in the gap was made experimentally. With the pressure of a gas mixture increased by a factor of 1.5, the time resolution did not change with the accuracy of 10% at the same overvoltage. With the spark gap increased by factor of 1.85, the time resolution measured with the same accuracy changed in proportion with the time delay (4). The results of these experiments show slower compared with $\sqrt{\bar{N}}$ dependence of the delay time fluctuation on $\bar{N}$.

The time resolution and delay time dependences on voltage applied to electrodes are given in Fig. 4. One can see, that the ratio of delay time to the time resolution is approximately constant and both are changing very rapidly with the voltage increase. However, when the high voltage is about two times higher than its threshold value the main discharge from particle is accompanied by afterpulses, and their number increases rapidly with the high voltage.

The model explaining all our experimental results consists in the assumption that the avalanches serie develop in the region around the main discharge, where the electric field is small, which results in the discharge in the region where the voltage is above its threshold value (Fig. 5). According to this model the initial electrons, appear from the cathode under influence of low energy photons (220-250 nm) where the gas mixture has no absorption (Fig. 2). These photons couldn't ionize the gas molecules, since their energy is less than ionization potential. Experimental facts explaining by this model, consist in the following.

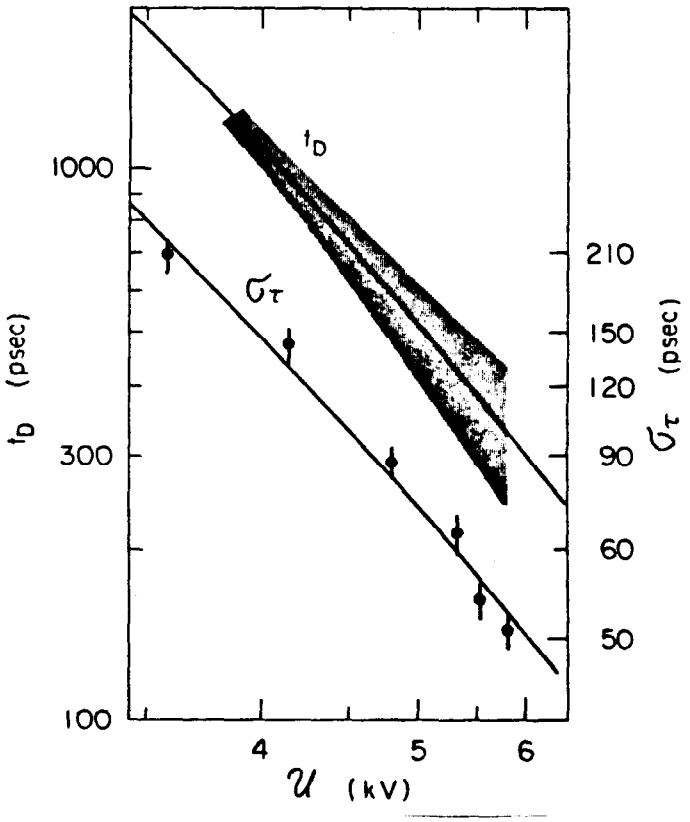

Fig. 4 The delay time t_D and time resolution σ_τ versus the voltage $\mathcal{U}$ for the spark counter with the 0,2 mm gap.

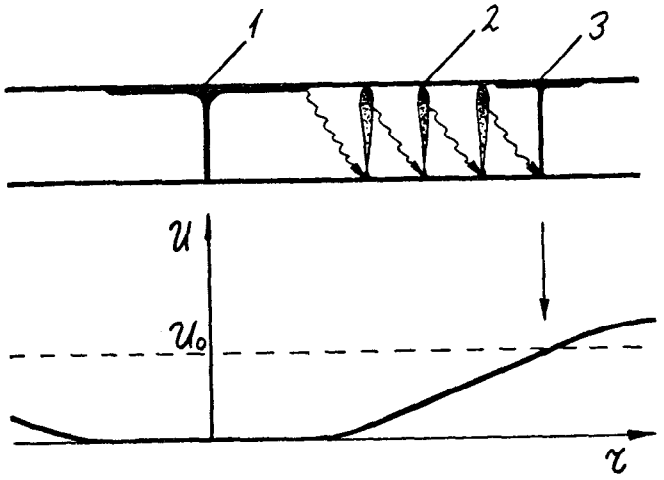

Fig. 5 The model of the afterpulse: 1 - the main discharge, 2 - avalanches serie, 3 - the afterpulse. The curve shows the high voltage distribution on the distance of the main discharge. $\mathcal{U}_0$ - the threshold voltage.

1. The number of afterpulses does not increase with increasing the absorption component pressure ($\lambda < 220$ nm).

2. The average delay time between the main pulse and the afterpulse $\Delta\tau \sim 100$ ns (Fig. 6) one can explain with the time necessary for the electron avalanches serie creation in a low electric field.

3. The afterpulse amplitude is less than the main pulse amplitude, since it takes place in the electric field about threshold value.

4. The dependence of afterpulses frequency on the properties of polymer film on the electrode surface was observed.

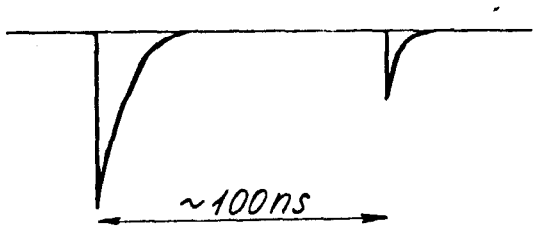

Fig. 6 A main pulse with afterpulse.

The gas mixture, used in the counter, has no absorption for the photons with the wavelengths ranging from 220nm to the photoeffect red boundary for an copper cathode. For the first turn-on of counter after its assembly, the "burning-in" period is required to obtain the localized discharge. This is accomplished using an intense radioactive source, and at the same time, high voltage is slowly increased. During this initial period of use, the electrode surfaces are coated with a film of polymerized gas, changing the work function of electrodes and localizing discharge. The properties of this film depend on the gas mixture. As was shown, the adding of a small quantity of diethyl ether results in the film formation, which reduces the number of afterpulses and enables to reach the higher overvoltage and hence to improve the time resolution. The time distribution of events with cosmic particles obtained for two counters with 0,1 mm spark gaps and each 11x11 cm^2 in size, is shown in Fig. 7. The

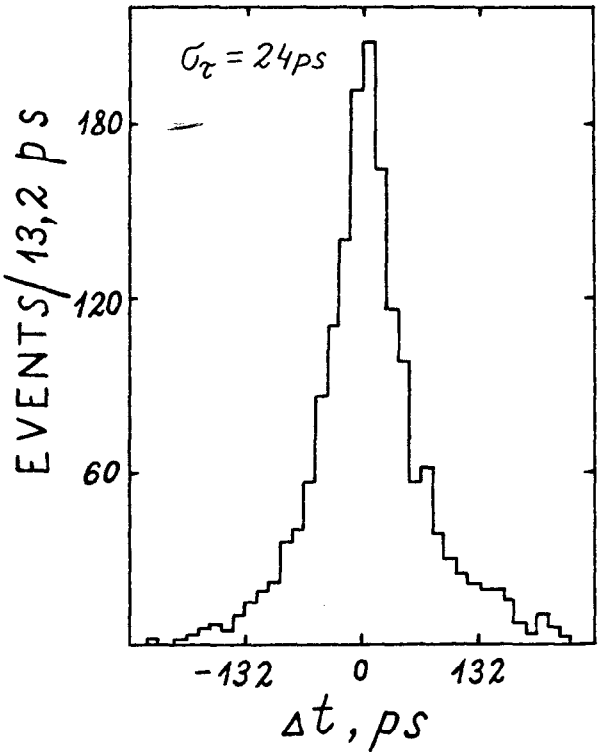

Fig. 7 Distribution of the time difference of two spark counters.

gas mixture contained 2,5% 1-3 butadiene, 1,9% ethylene, 3.3% diethyl ether, 6.6% isobutane, 85.1% neon under the total pressure of 12 atm. The counter time resolution of σ_τ = 24 ps was obtained at an operating voltage 4.5 kV, (the threshold for ionizing radiation to produce discharges was U_0 = 1.97kV). Obviously, the creation of film with higher work function results in further improvement of time resolution.

The full solution of the problem will be using the gaseous admixture absorbing the photons in $220 < \lambda < 250$ nm range. Our search in this direction does not give us a positive result yet. When this problem will be solved, one can expect the improvement of counter time resolution to $\sigma_\tau \sim 8$ ps due to increasing the electric field at a factor of two above the previous value. It is supposed that electric field strength of E ≃ 1 MeV/cm is still too low to produce autoelectron emission from cathode.

3. The Measurement of the Pion Form Factor

The Localized-discharge spark counters were used for the first time in the experiments on measuring the pion form factor near $e^+e^- \to \pi^+\pi^-$ reaction threshold at the VEPP-2M facility (Novosibirsk) [5]. A time-of-flight spectrometer in Fig. 8 has been designed on the basis of these counters with 0.1 mm spark gap. Two spark counters of 11 cm x 11 cm and 30 cm x 30 cm in size were located at a distance of 12 cm and 62 cm in a vertical plane on both sides of the beam interaction region. They were used for measuring the time of flight and coordinates of the collinear pairs of the produced particles.

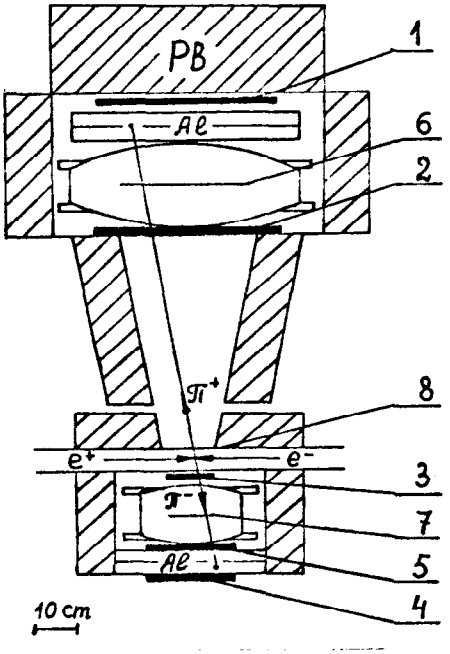

Fig. 8 General view of time of flight spectrometer: 1÷5 - scintillation counters; 6,7 - upper and lower spark counters, 8 - wall of vacuum chamber of VEPP-2M storage device.

Scintillation counters were utilized as range counters since the pions stopped in an aluminium absorber not reaching scintillation counters 1 and 4. The event distribution over time delay between the passage of the collinear pairs through the spark counters at an energy of 2 x 219 MeV for the particles which are not registered in scintillation counters 1 and 4 is shown in Fig. 9. The delay time between two peaks, $\Delta\tau \sim 500$ psec, corresponds to the time of flight difference for electrons and pions over the 50 cm differential flight path of the spectrometer.

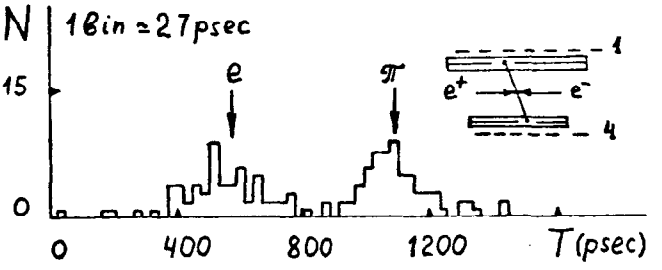

Fig. 9 The event distribution over time delay between operation of two spark counters with no signal from scintillation counters 1 and 4.

For this experiment the gas mixture mentioned earlier was used. The operating voltage was such that the resolution $\sigma_\tau \simeq 50$ ps for each counter. The specific feature of a spectrometer was the absence of conventional traking chambers, their role was played by spark counters. In this experiment the pion form factor near the $e^+e^- \to \pi^+\pi^-$ reaction threshold was measured, an electromagnetic pion mean square radius, $\langle r_\pi^2 \rangle = 0.37 \pm 0.05$ f^2 was found, which is an agreement with the result $\langle r_\pi^2 \rangle = 0.31 \pm 0.04$ f^2 of the FNAL-Dubna πe - scattering experiment /6/. The data collection for this experiment lasted for about 60 days.

4. Status of the spark counter program in Novosibirsk

The typical sizes of detectors for large physical devices are of 2÷3 meter. Our estimations and experiments have shown that the manufacturing of spark localized-discharge counters of such sizes seemed to be quite realistic. The main difficulties confronted are due to the preparation of the large, fine, nondefective electrode surfaces before assembly of counters. To find the principal solution of this problem, we are currently constructing a counter of 90 cm long. This counter will be composed of three sections connected in series, each 11 x 30 cm in size.

The other important problem is to find new gas mixtures with better time characteristics and less prone to polymerization induced by the discharges.

The comparison of various nobel gases influence on the counter characteristics was made. Neon compared to Ar and Xe decreases the threshold value and has good time resolution. The low operating voltage should improve the gas mixture stability. The search of the new absorption admixture, according

to the above mentioned principles, is in progress now.

To our opinion, the advantage of these detectors are the high time and coordinate resolutions in combination with an ease of signal processing, using time-amplitude converters. Moreover, since each particle discharges a small region of the counter, the signal amplitude of several particles is proportional to the number of particles. This may enable one to design electromagnetic shower and hadron calorimeters on the basis of localized discharge spark counters.

References

1. V.V.Parchomchuck, Yu.N.Pestov, N.V.Petrovykh, Nucl. Instr. and Meth., 93, 269 (1971).
   V.D.Laptev, Yu.N.Pestov, N.V.Petrovykh, Pribory i Tekh. Eksperim., 6, 36 (1975).
   A.D.Afanas'ev, V.D.Laptev, Yu.N.Pestov, B.P.Sannikov, Pribory i Tekh Eksperim., 6, 39 (1975).
   V.D.Laptev, Yu.N.Pestov, Pribory i Tekh. Eksperim., 6, 41 (1975).
   Yu.N.Pestov, G.V.Fedotovich, Preprint IYAF 77-78, Novosibirsk, (1977).
   V.D.Laptev, Yu.N.Pestov et al. Izv. Akad. Nauk SSSR, 42, 1488 (1978).
2. Yu.N.Pestov, N.V.Petrovykh, The certificate of author, USSR, N 349651 (1971).
3. Raether H. "Electron Avalanches and Breakdown in Gases". Butterworth's, London (1964).
4. Kalashnikova V.I., Kosodaev M.S. Elementary Particles Detectors". Nauka, Moscow (1966).
5. I.B.Vasserman, P.M.Ivanov, Yu.N.Pestov et al., Yadernaya Fizika, 33, 709 (1981).
6. E.B.Dally, D.J.Drickey et al., Phys. Rev. Lett., 39, 1176 (1977).